

Received: 2018.10.09

Accepted: 2019.01.11

Published: 2019.06.22

Levetiracetam Protects Against Cognitive Impairment of Subthreshold Convulsant Discharge Model Rats by Activating Protein Kinase C (PKC)-Growth-Associated Protein 43 (GAP-43)-Calmodulin-Dependent Protein Kinase (CaMK) Signal Transduction Pathway

Authors' Contribution:
Study Design A
Data Collection B
Statistical Analysis C
Data Interpretation D
Manuscript Preparation E
Literature Search F
Funds Collection G

BCDEF 1,2,3,4
ABCDEF 2,3,4,5
BCDF 3,5
BCF 3,5

Min-Jian Wang
Li Jiang
Heng-Sheng Chen
Li Cheng

1 Department of Psychology, Children's Hospital of Chongqing Medical University, Chongqing, P.R. China
2 Ministry of Education Key Laboratory of Child Development and Disorders, Chongqing, P.R. China
3 Key Laboratory of Pediatrics in Chongqing, Chongqing, P.R. China.
4 Chongqing International Science and Technology Cooperation Center for Child Development and Disorders, Chongqing, P.R. China.
5 Department of Neurology, Children's Hospital of Chongqing Medical University, Chongqing, P.R. China

Corresponding Author: Li Jiang, e-mail: wjmjmaster@hainan.net
Source of support: Departmental sources

Background: Subclinical epileptiform discharges (SEDs) are defined as epileptiform electroencephalographic (EEG) discharges without clinical signs of seizure in patients. The subthreshold convulsant discharge (SCD) is a frequently used model for SEDs. This study aimed to investigate the effect of levetiracetam (LEV), an anti-convulsant drug, on cognitive impairment of SCD model rats and to assess the associated mechanisms.




Material/Methods: A SCD rat model was established. Rats were divided into an SCD group, an SCD+ sodium valproate (VPA) group, and an SCD+ levetiracetam (LEV) group. The Morris water maze was used to evaluate the capacity of positioning navigation and space exploration. The field excitatory post-synaptic potentials (fEPSPs) were evaluated using a bipolar stimulation electrode. NCAM, GAP43, PS95, and CaMK II levels were detected using Western blot and RT-PCR, respectively. PKC activity was examined by a non-radioactive method.

Results: LEV shortens the latency of platform seeking in SCD rats in positioning navigation. fEPSP slopes were significantly lower in the SCD group, and LEV treatment significantly enhanced the fEPSP slopes compared to the SCD group ($P<0.05$). The NCAM and GAP-43 levels were increased and PSD-95 levels were increased in SCD rats ($P<0.05$), which were improved by LEV treatment. The PKC activity and CaMK II levels were decreased in SCD rats and LEV treatment significantly enhanced PKC activity and increased CaMK II levels.

Conclusions: Cognitive impairment in of SCD model rats may be caused by decreased PKC activity, low expression of CaMK II, and inhibition of LTP formation. LEV can improve cognitive function by activating the PKC-GAP-43-CaMK signal transduction pathway.

MeSH Keywords: **Calcium-Calmodulin-Dependent Protein Kinase Type 1 • Cognition • Convulsants**

Full-text PDF: <https://www.medscimonit.com/abstract/index/idArt/913542>

 4626  1  7  58



Background

Subclinical epileptiform discharges (SEDs) were defined as epileptiform electroencephalographic (EEG) discharges without clinical signs of seizure in patients [1,2]. The partial and generalized epileptiform EEG discharges can be subclinical, but even short-duration SEDs lasting only 0.5 s can damage cognition [3]. The positive rate of SEDs in normal children is 1.9% to 5.0%, and achieves higher levels in children with neuro-developmental disorders such as attention deficit hyperactivity disorder (ADHD), autism spectrum disorder, and mental development disorders [4,5]. Recent studies [6,7] proved that SEDs induce cognitive impairment in animal models and in human patients.

The animal model of the SEDs uses subthreshold convulsant discharge (SCD), which has been extensively used and accepted in research [8,9]. However, the role of the long-term potentiation (LTP) in the pathogenic process of SCD has not been investigated. TLP is a type of synaptic plasticity, which refers to the signal transmission enhancement at a synapse and results from coordinated activity of at least 2 neurons [10,11]. LTP is also considered as the neurological basis for memory and learning, and are associated with cognitive functions [12]. To the best of our knowledge, this is the first study to explore the therapeutic effects of anti-epileptic drugs. Use of anti-epileptic drugs to treat SEDs patients is controversial. Therefore, we performed the present study to assess the correlation between LTP and SEDs.

The neural cell adhesion molecule [13], post-synaptic density (PDS-95) [14], and growth-associated protein 43 (GAP-43) [15] are closely correlated with differentiation, migration, and regeneration of the central nervous system, are associated with the synaptic connection, and also are involved in cognitive disorders [16]. The calmodulin-dependent protein kinase II (CaMK II) and protein kinase C (PKC) have been reported to be involved in the induction and maintenance of central sensitization [17]. CaMK II is a multifunctional serine/threonine protein kinase in neurons, which is also believed to regulate neurotransmission and synaptic plasticity [18]. Fluctuations in CaMK II activity are associated with excitotoxic calcium dysregulation in neuronal diseases such as the epilepsy, stroke, and traumatic brain injury [19]. Liu et al. [20] suggested that hippocampal PKC isoforms play different roles in seizure generation, and may be targets for the development of anti-convulsive drugs. Yabuki et al. [21] also reported that decreased CaMK II and PKC activities are associated with cognitive impairment.

Sodium valproate (VPA) and levetiracetam (LEV) are extensively used anti-epileptic drugs in clinical practice, and both have satisfactory therapeutic effects and safety [22,23]. VPA plays an anti-epileptic role, mainly by enhancing the inhibitory

neurotransmitter gamma aminobutyric acid (GABA) [24], and LEV plays an anti-epileptic role by combining synaptophysin with synaptic vesicle protein 2A (SV2A) [25].

We used the Morris water maze test to study rat behavior, examined rat hippocampal slices LTP to observe the electrophysiology, and evaluated NCAM, PSD-95, and GAP43 to investigate the synaptic plasticity, as well as accessing changes in CaMK II and PKC activities. Finally, we explored the therapeutic effects of VPA and LEV on the SCD model rats by detecting the above biomarkers.

Material and Methods

Animals

We obtained 64 specific pathology-free (SPF) Sprague-Dawley (SD) rats (210±10 g, 3 months, male, certificate No. SYXK-[Chongqing]-2012-0015) from the Experimental Animal Center of Chongqing Medical University, Chongqing, China. The rats were housed in an environment with a light/dark cycle of 12 h/12 h at room temperature. The rats had free access to food and water. The animal experiments were completed by the professional animal experimental staff (certificate No. CQLA-2013-0027). All experiments were approved by the Ethics Committee of Chongqing Medical University, Chongqing, China.

Establishment of subthreshold convulsant discharge rat model

Electrode implantation: All of the SD rats were anesthetized by intraperitoneal injections of 10% chloral hydrate (1 mg/kg). Localizer ear levers were inserted into the 2 external auditory canals, with the symmetrical scale. Surgery for electrode implantation was performed according to a previously published study [26]. The rats were placed in a stereotaxic apparatus (Stolting USA), and 4 electrode implantation positions were selected as described in a previous study [27]. The 4 electrodes were: a hippocampal stimulating electrode (4.2 mm behind the anterior fontanelle, right lateral opening for 2.0 mm), a cerebral cortex recording electrode 1 (2.5 mm on the front of anterior fontanelle, left lateral opening for 2.0 mm), a cerebral cortex recording electrode 2 (5.0 mm on the front of anterior fontanelle, left lateral opening for 3.5 mm), and an earth electrode (2.5 mm on the front of anterior fontanelle, right lateral opening for 2.0 mm). Then, a hole was drilled into the skull, and a probe was implanted into the 4 electrode implantation positions.

For the electrical stimulation program, the parameters were wave width 1 ms, frequency 30 Hz, string length 10 s, with constant current and unidirectional wave, 10 times every day for 4 days. In this study, we used a stimulus intensity of 0.02 mA,

0.04 mA, 0.06 mA, and 0.08 mA to stimulate the rats. Ten rats underwent stimulus intensity testing.

For subthreshold convulsant discharge judgment, the rat convulsions were divided into 5 grades according to a previous study [28]: stage 0 (no abnormality), stage 1 (mouth and facial movements), stage 2 (head nodding), stage 3 (forelimb clonus), stage 4 (rearing), and stage 5 (rearing and falling). Full motor seizure followed by temporary loss of postural control was considered as stage 5 motor seizure.

EEG recording

One week after the surgery, EEG signals were recorded using a special animal electroencephalograph (AD instruments, Castle Hill, Australia). The voltage differential between the pair of electrodes in both hemispheres were amplified using a high-pass filter and recorded. The videos were recorded at 30 frames/s, and the EEG signals were sampled at 400 Hz.

Trial grouping and drug administration

The 64 rats were divided into 4 groups: a normal group (only 4 electrode were implanted, without electrical stimulation), an SCD group (subthreshold convulsant discharge rat model), an SCD+VPA group (the subthreshold convulsant discharge rat model was intragastrically VPA, 150 mg/kg/d [29], 2 times per day for 28 days), and an SCD+LEV group (the subthreshold convulsant discharge rat model was intragastrically LEV, 150 mg/kg/d [30], 2 times per day for 28 days). Both VPA and LEV were dissolved in sterile 0.9% saline. Our preliminary findings indicated that 150 mg/kg/d LEV is the optimal dosage used (data not shown). VPA was purchased from Sanofi (Westborough, MA, USA) and LEV was purchased from UCB Pharma (Brussels, Belgium).

Morris water maze test

The Morris water maze system was purchase from Beijing Sunny Instruments Co. (Beijing, China), which was composed of a circular pool, a platform, a video camera, a displayer, and video tracking software. Behavioral training and testing were conducted in a circular pool (diameter 150 cm, depth 80 cm), and maintained at a temperature of 20–22°C. Four geometrical figures (northwest, northeast, southwest, southeast) in black and white (approx. 20 cm wide) were attached to the upper rim of the pool. The platform (12 cm wide) was 1 to 2 cm under the water surface. The animal movements were monitored and recorded using a video camera (Beijing Sunny Instruments Co., Beijing, China) mounted above the pool. The behavioral data were recorded and analyzed using Morris water maze video tracking software (Beijing Sunny Instruments Co., Beijing, China).

The whole process was divided into 2 stages – positioning navigation and space exploration – performed according to previously studies [31,32].

Nine (or 23) days after drug treatment, the rats in all 4 groups (8 rats per group) underwent the pre-experiment of positioning navigation to acquaint them with the test apparatus and locations. Ten (or 24) days after drug treatment, the positioning navigation test was formally performed, and continued for 4 days. Then, the space exploration test was performed 14 (28) days after the drug treatment.

Hippocampal slices and LTP recording

Fourteen days after the drug treatment, in every group (n=8), the hippocampal slices were prepared and maintained according to the previous published study [33]. In brief, the hippocampal slices with the thickness of 300 to 400 µm were maintained for 1 h prior to being transferred to a chamber filled with artificial cerebrospinal fluid (ACSF). ACSF contains 124 mM NaCl, 5 mM KCl, 1.25 mM NaH₂PO₄, 1 mM MgCl₂, 2 mM CaCl₂, 26 mM NaHCO₃, and 10 mM glucose. Then, the ACSF was adjusted to pH 7.4, and incubated with 95% O₂ and 5% CO₂. Finally, the hippocampal slices were superfused with ACSF at flow a rate of 1.5 ml/min at 35°C for 40 min.

The field excitatory post-synaptic potentials (fEPSPs) were evaluated by using a bipolar stimulation electrode (200 µm diameter, Worcester Polytechnic Institute, MA, USA), and results were recorded using glass microelectrodes (1–2 MΩ) filled with ACSF from the *stratum radiatum* of the CA1 region. The initial pulse stimulation intensity was adjusted to evoke 50% of the maximal response of fEPSP. When the fEPSP slope increased by 20% or more, and recorded a stable baseline for at least 30 min, the LTP was considered as successfully induced and established. The recordings were filtered at 100 Hz and digitized at 500 Hz by using Igor Pro (WaveMetrics Inc., Lake Oswego, OR, USA). In slices obtained from rats during behavioral experiments, paired pulses of 30-ms intervals were applied during the entire LTP protocol [34].

The data of LTP slope reflected the values of fEPSP in every group; a higher LTP slope was associated with a higher fEPSP and better synaptic plasticity [35]. We recorded the induced LTP at 2 time points: 1 min and 30 min after the high-frequency stimulation (HFS).

Hippocampal samples preparation

The hippocampal samples were extracted after 14 days and 28 days of drug treatment. The SD rats in every group were anesthetized by intraperitoneal injection with 10% chloral hydrate (1 ml/kg). The rats were decapitated, the brain tissues

Table 1. The primer sequences for the real-time PCR.

Genes	Primer sequences	Length (bp)	Annealing temperature (°C)
β-actin	Forward: 5'-CAGTGCCAGCCTCGTCTCAT-3'	150	60
	Reverse: 5'-AGGGGCCATCCACAGTATTC-3'		
NCAM	Forward: 5'-GCCTGGAACCAATACTACAT-3'	364	56
	Reverse: 5'-ACAGTCGGCTCAGAATACCC-3'		
GAP43	Forward: 5'-GGCTCTGCTACTACCGATCC-3'	185	58
	Reverse: 5'-TTGGAGGACGGCGAGGTTA-3'		
PSD-95	Forward: 5'-CATCGCCATCTTCATCCGTC-3'	148	55
	Reverse: 5'-TCAAAGCTGTCGCCCTCTAC-3'		
CaMKIIα	Forward: 5'-CTGAACCCTCACATCCACCT-3'	189	58
	Reverse: 5'-ATCTGCCATTTCCATCCCT-3'		

were isolated, and the hippocampal tissues were extracted. Then, the hippocampal tissues were homogenized in ice-cold homogenization buffer containing 300 mM protease inhibitor (Sigma-Aldrich, St. Louis, MO, USA), 10 mM HEPES, and adjusted to pH 7.5 by using the Ultra-Turrax system (IKA, Staufen, Germany). The homogenate was then centrifuged at 4000 rpm for 5 min using a HimacCF15 low-temperature and high-speed centrifuge (Hitachi, Tokyo, Japan), and the pellets were discarded. Then, the protein concentration and content were evaluated using bicinchoninic acid (BCA) protein assay kit (Tiangen Biotech Co., Beijing, China) according to the manufacturer's instruction. The extracted hippocampal proteins were aliquoted and stored at -80°C for further tests.

Western blot assay

A total of 0.2 μg extracted hippocampal proteins were separated by using 15% SDS-PAGE (Sigma-Aldrich, St. Louis, Missouri, USA) and electro-transferred onto the PVDF membranes (Millipore, Boston, MA, USA). The PVDF membranes were blocked using the 5% defatted milk for 2 h at 4°C overnight. The PVDF membranes were incubated with rabbit anti-rat NCAM polyclonal antibody (Catalogue No: GTX133217, 1: 2000, GeneTex, Inc., Alton Pkwy Irvine, CA, USA), mouse anti-rat GAP43 monoclonal antibody (Catalogue No. GTX34384, 1: 3000, GeneTex, Inc.), mouse anti-rat PSD-95 monoclonal antibody (Catalogue No. MABN68, 1: 3000, Millipore, Boston, MA, USA), mouse anti-rat CaMK II monoclonal antibody (Catalogue No. sc-5306, 1: 3000, Santa Cruz Biotech), and mouse anti-β actin monoclonal antibody (Catalogue No. GTX11003, 1: 3000, GeneTex Inc.) for 2 h at room temperature. The membranes were then incubated with horseradish peroxidase (HRP)-conjugated goat anti-rabbit IgG (Catalogue No. sc-2005, 1: 2000, Santa Cruz Biotech.) and goat anti-rabbit IgG (Catalogue No. sc-2004, 1: 2000, Santa Cruz Biotech) at 37°C for 1 h. Finally, the Western blot bands were visualized with an enhanced chemiluminescent (ECL) kit (Sigma-Aldrich, St. Louis, MO, USA).

Real-time RT-PCR assay

Total RNAs of the hippocampal tissues were extracted using TRIzol reagents (Tiangen Biotech Co., Beijing, China). Then, the KI1622 Reverse Transcription kit (Thermo Electron Corp, Waltham, MA, USA) was utilized to synthesize the cDNAs according to the manufacturer's instructions. The synthesized cDNA was amplified as the templates by using the Sybgreen qPCR kit (Tiangen Biotech Co.) as the fluorescent dye, and performed with the real-time PCR system (MJ ReSCarch Inc., St. Bruno, Quebec, Canada). Then, the following conditions were used for amplification: 95°C for 2 min, 95°C for 10 s, 60°C for 15 s, 72°C for 45 s, and for 40 cycles. The primers for the NCAM, GAP43, PSD-95, CaMK II, and β-actin are listed in Table 1. Finally, the amplified products were loaded onto 1.5% agarose gels, and the images were analyzed using Quantity One image analysis software (Bio-Rad Laboratories, Hercules, CA, USA). The relative mRNA expression of target genes was normalized to the β-actin gene using the comparative threshold cycle ($2^{-\Delta\Delta\text{CT}}$) method. Amplification and melting curves (data not shown in figures) were drawn.

PKC activity examination

PKC activity was examined by a non-radioactive method according to a previously published study [36]. Briefly, hippocampal tissues were lysed in 1000 μl PKC extraction buffer (1 μg/ml leupeptin [Sigma-Aldrich], 1 μg/ml aprotinin [Sigma-Aldrich], 25 mM Tris [Sigma-Aldrich], 10 mM mercaptoethanol [Sigma-Aldrich], 10 mM β-mercaptoethanol [Sigma-Aldrich], 0.05% Triton X-100 [Sigma-Aldrich], 0.5 mM EDTA [Sangon, Shanghai, China], and 0.5 mM EGTA [Sangon]). Equal amounts of hippocampal tissue proteins were utilized in each PKC reaction according to the protocol of the PepTag® non-Radioactive Protein Kinase C detection kit (Promega, Madison, WI, USA). The hippocampal tissue samples were then incubated with a fluorescent, positively-charged, PKC-specific peptide

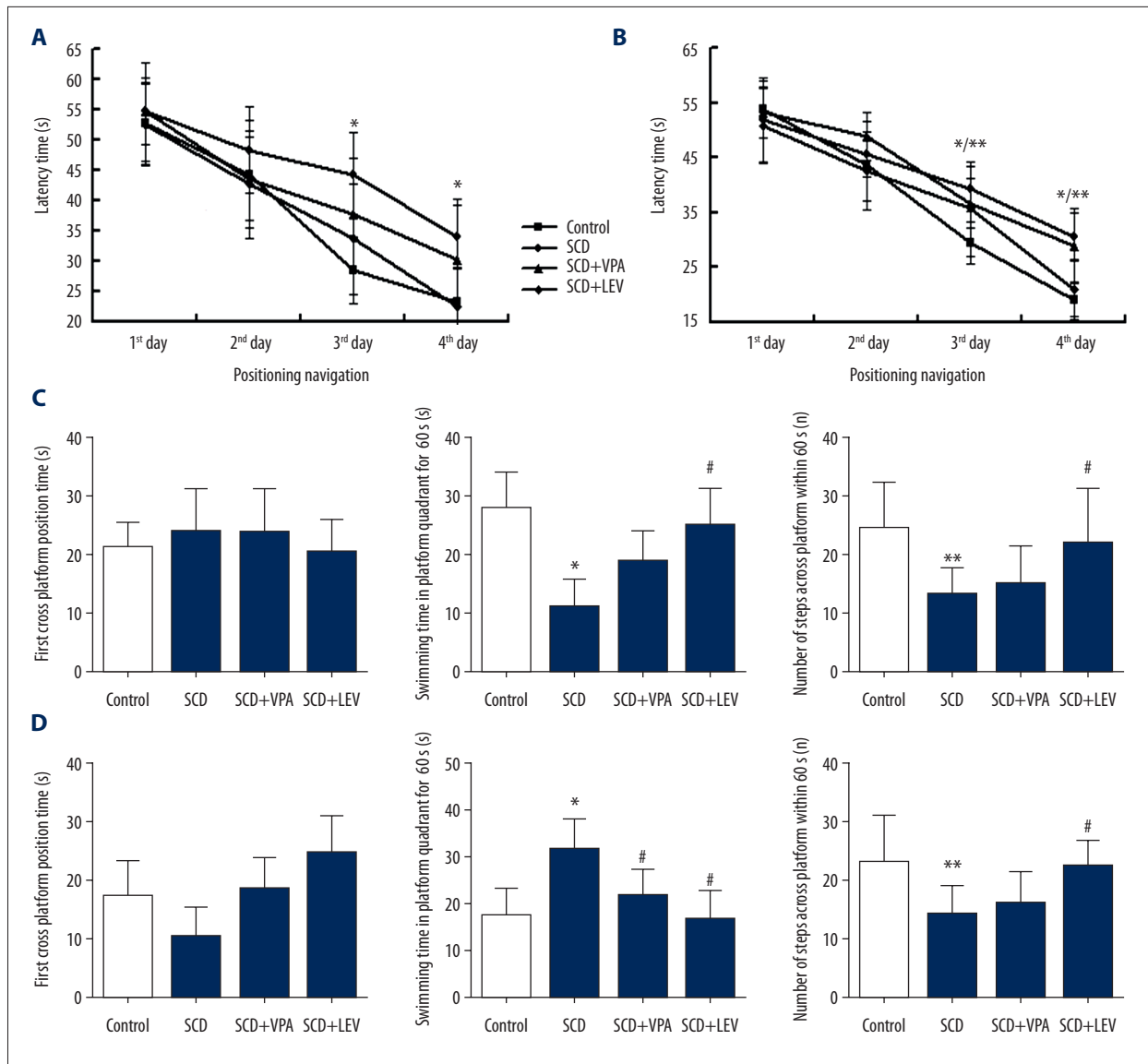


Figure 1. Latency of platform seeking in positioning navigation and spatial probe test data at 14 days or 28 days after intragastric administration (n=64). **(A, B)** Latency of platform seeking in positioning navigation at 14 and 28 days after intragastric administration. **(C, D)** Spatial probe test data at 14 days or 28 days post intragastric administration. * P<0.05, ** P<0.01 vs. Control group, # P<0.05 vs. SCD group. Dose of VPA: 150 mg/kg/d, dose of LEV: 150 mg/kg/d.

(C1 peptide, 0.4 µg/µl) for 30 min and separated on 0.8% agarose gels. The phosphorylated, negatively-charged peptide was separated from non-phosphorylated, positively-charged peptide and visualized under UV light. The bands were quantified by densitometry and normalized to the controls.

Statistical analysis

Data in this study were analyzed using SPSS software 117.0 (SPSS Inc., Chicago, IL, USA). Data are described as mean ± standard deviation (SD). All of the data were obtained from at least 3 independent tests or experiments. One-way ANOVA was used

to assess differences between 2 or more different groups. For comparisons between 2 groups, the *t* test was used. A P<0.05 value was considered as the level of statistical significance.

Results

LEV shortens the latency of platform seeking in positioning navigation

There were no significant differences in latency of platform seeking among the 4 groups on the first day and second day of

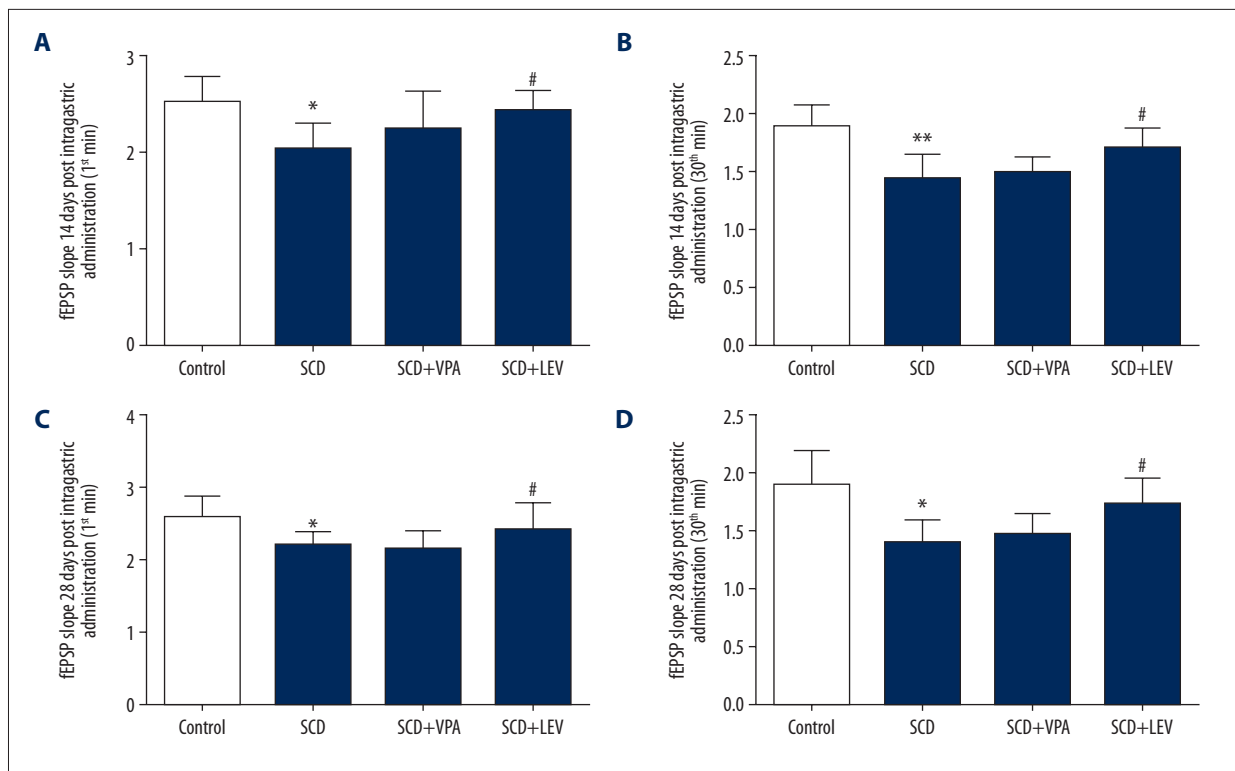


Figure 2. fEPSP slope at 14 days (A, B) and 28 days (C, D) after intragastric administration, both 1 min after HFS and 30 min after HFS (n=64). * P<0.05, ** P<0.01 vs. Control group, # P<0.05, ## P<0.05 vs. SCD group. Dose of VPA: 150 mg/kg/d, dose of LEV: 150 mg/kg/d.

14 days (Figure 1A) and 28 days (Figure 1B) after intragastric administration ($P>0.05$). However, there were significant differences in the latency of platform seeking among the 4 groups on the third day and fourth day of 14 days (Figure 1A) and 28 days (Figure 1B) after intragastric administration ($P<0.05$). The latency of platform seeking in the SCD group was longer significantly compared to the Control group at both 14 days (Figure 1A) and 28 days (Figure 1B) after intragastric administration ($P<0.01$ on the third day, $P<0.05$ on the fourth day). The latency of platform seeking of the SCD+LEV group (LEV treatment) was significantly shorter compared to the SCD group at 14 days (Figure 1A) and 28 days (Figure 1B) after intragastric administration ($P<0.01$ on the third day, $P<0.05$ on the fourth day). Furthermore, we found that the VPA did not affect the latency of platform seeking at 14 days or 28 days after intragastric administration.

LEV improved the spatial probe test results

There were no significant differences for the first platform-crossing time among the 4 groups at 14 days (Figure 1C) or 28 days (Figure 1D) after intragastric administration ($P>0.05$). Swimming time in the platform quadrant for 60 s in the SCD group was significantly lower compared to the Control group at 14 days (Figure 1C) and significantly higher compared to the

Control group at 28 days (Figure 1D) after intragastric administration ($P<0.05$). The LEV treatment (SCD+LEV group) significantly prolonged the swimming time in the platform quadrant at 14 days (Figure 1C), but significantly shortened the swimming time compared to the SCD group at 28 days (Figure 1D) after intragastric administration ($P<0.05$). The number of times crossing the platform within 60 s in the SCD group was significantly fewer compared to the Control group both at 14 days (Figure 1C) and 28 days (Figure 1D) after intragastric administration ($P<0.05$). The LEV treatment (SCD+LEV group) significantly increased the number of times crossing the platform within 60 s compared to the SCD group at 14 days (Figure 1C) and 28 days (Figure 1D) after intragastric administration ($P<0.05$).

LEV enhances the fEPSP slopes

One-way ANOVA showed that there were significant differences among the 4 groups for fEPSP slope at 14 days (Figure 2A, 2B) and 28 days (Figure 2C, 2D) after intragastric administration, both 1 min after HFS and 30 min after HFS. The fEPSP slopes were significantly lower in the SCD group compared to the Control group, and LEV treatment significantly enhanced the fEPSP slopes compared to the SCD group both at 14 days (Figure 2A, 2B) and 28 days (Figure 2C, 2D) after intragastric administration ($P<0.05$).

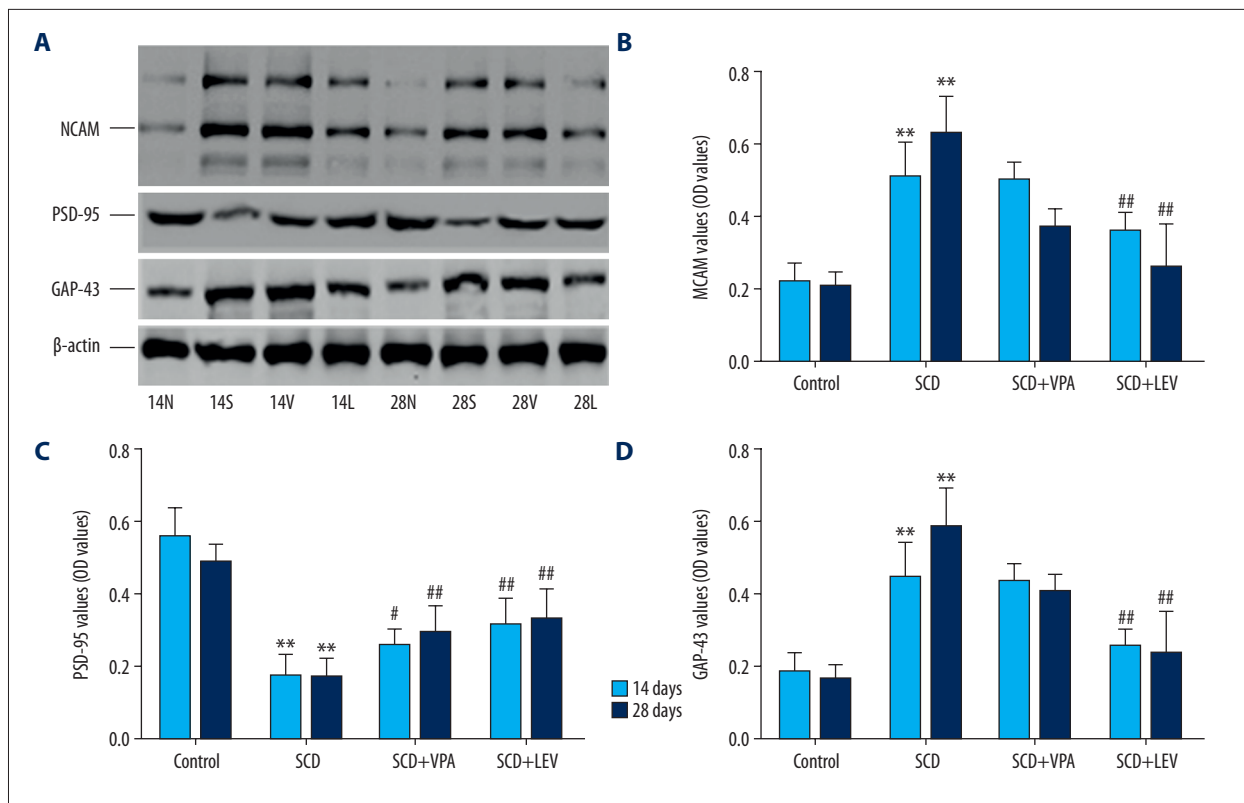


Figure 3. Evaluation of the expression of NCAM, PSD-95, and GAP-43 by Western blot assay (n=32). **(A)** Western blot bands for NCAM, PSD-95, and GAP-43 expression. **(B)** Statistical analysis of NCAM protein expression. **(C)** Statistical analysis of PSD-95 protein. **(D)** Statistical analysis of GAP-43 protein. * P<0.05, ** P<0.01 vs. Control group, # P<0.05, ## P<0.05 vs. SCD group. 14N (28N), 14S (28S), and 14L (28L) represent the Control group, SCD group, and SCD+LEV group, respectively, at 14 days (28 days) after intragastric administration. Dose of VPA: 150 mg/kg/d, dose of LEV: 150 mg/kg/d.

LEV decreases the levels of NCAM protein and mRNA

Western blot assay showed that the protein levels of NCAM were significantly increased in the SCD group compared to the Control group, both at 14 days and 28 days after intragastric administration (Figure 3A, 3B, both P<0.05). However, the LEV treatment significantly decreased levels of NCAM protein compared to the SCD group, both at 14 days and 28 days after intragastric administration (Figure 3A, 3B, both P<0.05). RT-PCR assay results also indicated that LEV significantly decreased the levels of NCAM mRNA compared to the SCD group at 14 days and 28 days after intragastric administration (Figure 4A, both P<0.05).

LEV increased the levels of PSD-95 protein and mRNA

Western blot results indicated that PSD-95 protein levels were significantly lower in the SCD group compared to the Control group, both at 14 days and 28 days after intragastric administration (Figure 3A, 3C, both P<0.05). However, LEV treatment significantly increased the levels of PSD-95 protein compared to the SCD group at 14 days and 28 days after intragastric

administration (Figure 3A, 3C, both P<0.05). The RT-PCR assay also showed that LEV treatment significantly increased the PSD-95 mRNA levels compared to the SCD group at 14 days and 28 days after intragastric administration (Figure 4B, both P<0.05).

LEV decreased expression of GAP-43

The Western blot results showed that the GAP-43 levels were significantly increased in the SCD group compared to the Control group, both at 14 days and 28 days after intragastric administration (Figure 3A, 3D, both P<0.05). However, LEV treatment significantly decreased the GAP-43 levels compared to the SCD group (Figure 3A, 3D, both P<0.05). RT-PCR assay also showed that LEV treatment significantly decreased the GAP-43 mRNA levels compared to the SCD group at 14 days and 28 days after intragastric administration (Figure 4C, both P<0.05).

LEV increased activity of p-PKC

The non-radioactive method for p-PKC activity (Figure 5A) indicated that activity of p-PKC was significantly decreased in the SCD group compared to the Control group at 14 days

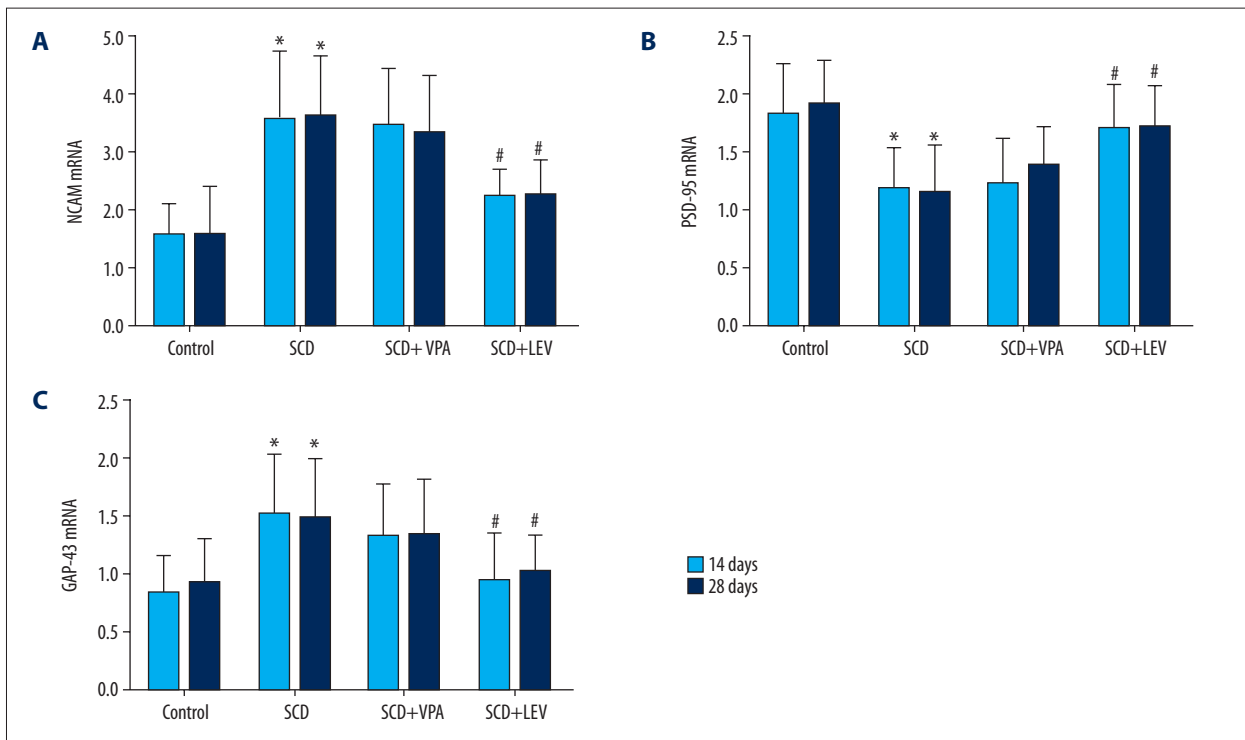


Figure 4. Observation for mRNA expression of NCAM, PSD-95, and GAP-43 by using RT-PCR assay (n=32). **(A)** Statistical analysis for NCAM mRNA expression. **(B)** Statistical analysis for PSD-95 mRNA expression. **(C)** Statistical analysis for GAP-43 mRNA expression. * P<0.05, ** P<0.01 vs. Control group, # P<0.05, ## P<0.05 vs. SCD group. 14N (28N), 14S (28S), and 14L (28L) represent the Control group, SCD group, and SCD+LEV group at 14 days (28 days) after intragastric administration, respectively. Dose of VPA: 150 mg/kg.d, dose of LEV: 150 mg/kg.d.

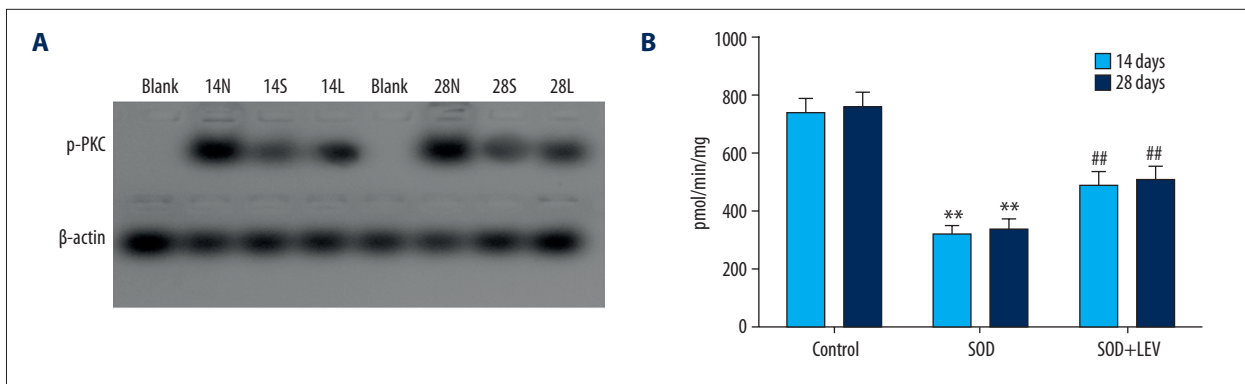


Figure 5. Examination for the p-PKC activity using a non-radioactive method (n=32). **(A)** The immunoblotting image. **(B)** Statistical analysis for p-PKC activity. ** P<0.01 vs. Control group, ## P<0.05 vs. SCD group. 14N (28N), 14S (28S), and 14L (28L) represent the Control group, SCD group, and SCD+LEV group at 14 days (28 days) after intragastric administration, respectively. Dose of VPA: 150 mg/kg/d.

and 28 days after intragastric administration (Figure 5B, both P<0.05). However, the LEV treatment significantly increased the p-PKC activity compared to the SCD group at 14 days and 28 days after intragastric administration (Figure 5B, both P<0.05).

LEV increased CaMK II levels

Western blot results showed that CaMK II levels were significantly decreased in the SCD group compared to the Control group at 14 days and 28 days after intragastric administration (Figure 6A, both P<0.05). However, LEV treatment significantly increased the levels of CaMK II levels compared

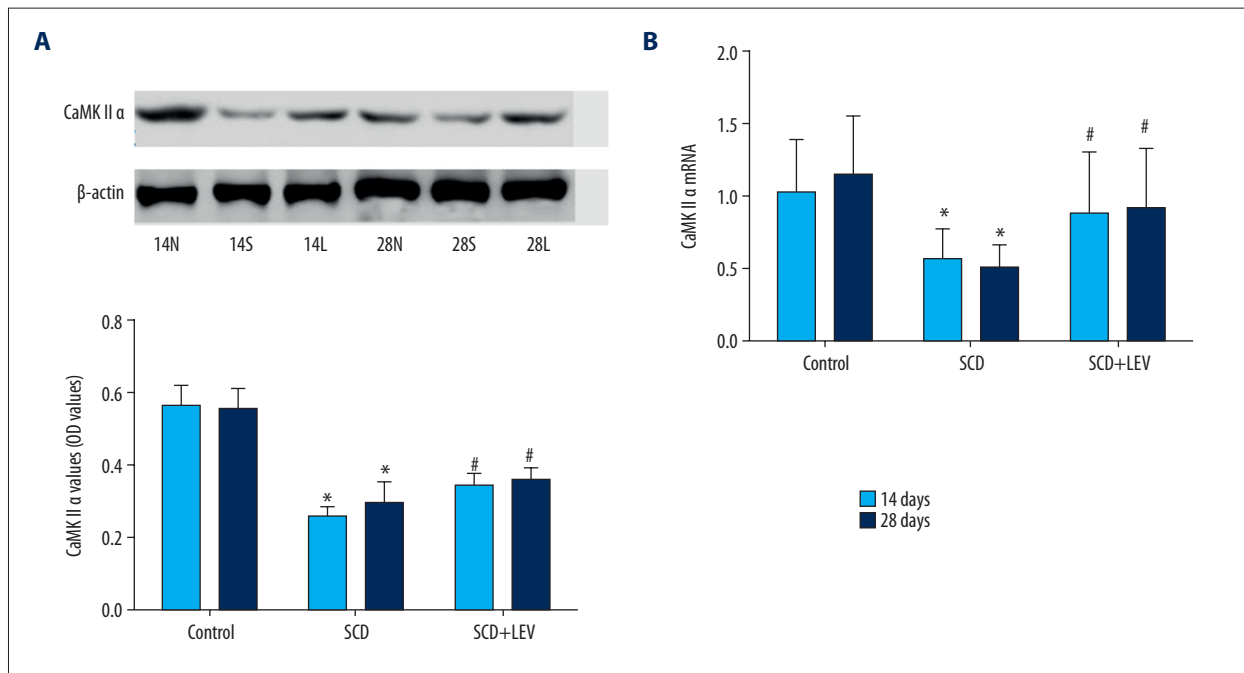


Figure 6. CaMK II expression was evaluated using both Western blot assay and RT-PCR assay (n=32). **(A)** Western blot assay and statistical analysis for CaMK II expression. **(B)** Statistical analysis for CaMK II mRNA expression. * P<0.05 vs. Control group, # P<0.05 vs. SCD group. 14N (28N), 14S (28S), and 14L (28L) represent the Control group, SCD group, and SCD+LEV group at 14 day (28 days) after intragastric administration, respectively. Dose of VPA: 150 mg/kg/d.

to the SCD group at 14 days and 28 days after intragastric administration (Figure 6A, both P<0.05). RT-PCR assay results also indicated that LEV treatment significantly increased the CaMK II levels compared to the SCD group at 14 days and 28 days after intragastric administration (Figure 6B, both P<0.05).

Discussion

In this study, we established the SCD using the electrical stimulation method, which has been extensively used by many scholars around the world [37]. We performed electrical stimulation in the hippocampus CA1 region to establish the SCD rat model, and the electrical stimulation parameter (0.06 mA stimulus intensity) was consistent with previous studies [38].

Cognitive function refers to the mental processes associated with acquisition of information, manipulation, knowledge, and reasoning, which includes the domains of the learning, memory, language, attention, and decision making [39]. Among these cognitive functions, learning and memory are most important. Therefore, we evaluated cognitive functions by examining the positioning navigation and space exploration, using methods previously described [40]. Our results indicated that the latency of platform seeking in positioning navigation was prolonged in the SCD model rats, but LEV shortens latency of platform seeking in positioning navigation at 14 days and 28 days

after intragastric administration. Furthermore, we found that VPA did not affect the latency of platform seeking after intragastric administration. The swimming time and, the number of times crossing the platform within 60 s suggest that the LEV clearly improves the learning and memory function, which is consistent with previously published studies [41,42]. Furthermore, we found that VPA did not affect cognitive functions of the SCD model rats at 14 days or 28 days after intragastric administration.

Synaptic plasticity is the changes in synaptic strength (the structures or the functions) produced by the diverse-stimulation procedures *in vitro* and *in vivo* [43]. Whitlock et al. [44] reported that synaptic plasticity is an important mechanism that underlies long-term memory storage. Therefore, synaptic plasticity is closely correlated to cognitive functions in model rats, which can be assessed through electrophysiology and synaptic function-associated proteins [45]. Long-term synaptic plasticity is usually divided into long-term potentiation (LTP, in which synaptic strength increases) and long-term depression (LTD, in which synaptic strength decreases). In this study, we found that fEPSP slopes were significantly lower in the SCD group compared to the Control group, and LEV treatment significantly enhanced fEPSP slopes compared to the SCD group after intragastric administration. These results suggest that LEV improves the LTP of SCD model rats, which is consistent with the Morris water maze test results.

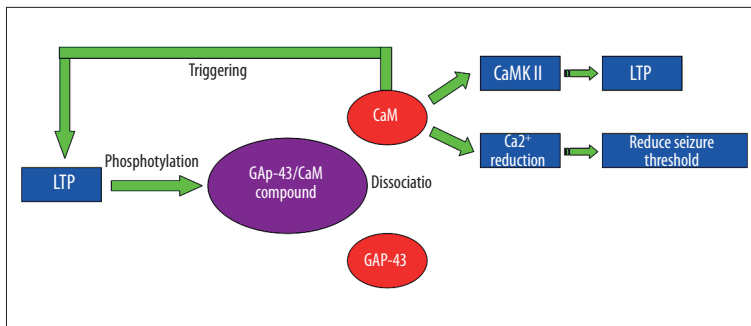


Figure 7. The signal pathway of PKC-GAP43-CaMK.

Many synaptic plasticity-associated proteins have been discovered, among which NCAM, PSD-95, and GAP-43 are closely correlated with LTP [46]. A previous study discovered that NCAM expression was obviously enhanced in the LTP induction period, and NCAM expression was blocked in the LTP maintenance period [47]. In the present study, the NCAM levels in hippocampal tissues of SCD rats were significantly increased, which suggests that subthreshold convulsant discharge damages the neurons. The mechanism may be similar to that in epilepsy, in which increased NCAM triggers formation of PSA-NCAM complex [48], which induces neuronal migration and nervous system re-contribution, and causes further cognitive impairment. The Morris water maze test and LTP results showed that cognitive function alterations are contrary to changes in NCAM, which also showed that overexpression of NCAM can affect the cognitive function of rats. We also found that LEV significantly decreased the NCAM expression in hippocampal tissues in SCD rats, but VPA did not trigger this change, which are consistent with the changes of NCAM in epilepsy-associated studies [49].

PSD-95 is composed of glutamate post-synaptic densities (PSDs) and participates in the signaling pathways that close the glutamate-gated ion currents [50]. Overexpression of PSD-95 significantly affects synaptic function, and the excitatory post-synaptic current is enhanced by up to 4-fold [51]. This increase triggers a strengthening process similar to that which occurs during LTP, in which the synapses strengthened by the overexpression of PSD-95 cannot finally be potentiated by the induction protocols of PSD-95 [52]. We found that PSD-95 proteins levels were significantly decreased in the SCD group compared to the Control group, and LEV treatment significantly increased the levels of PSD-95 protein compared to the SCD group. We speculate the mechanism may act by negatively regulating the sensitivity of NMDA to glutamate and decreasing the combination of NMDA and glutamate. However, this hypothetical mechanism needs to be proven in future research.

GAP-43 is a presynaptically distributed and growth-related protein, and its phosphorylation is enhanced after LTP [53]. The perforant path LTP alters the GAP-43 RNA expression in the intact freely moving rats after LTP induction [54]. The role of LEV in epilepsy in a rat model is controversial, either decreasing GAP-43

levels or increasing GAP-43 levels. In this study, we discovered that LEV treatment significantly decreased the GAP-43 levels compared to the SCD group, and VPA did not have this effect. This result suggests that LEV can decrease GAP-43 levels in SCD model rats, which is consistent with GAP-43 downregulation.

According to the changes in GAP-43 levels associated with LTP and synaptic plasticity, we speculated that the cognitive function-related PKC-GAP43-CaMK II-LTP signaling pathway participates in SCD (Figure 7). The PKC is an important intracellular signal transduction molecule, and its phosphorylation mediates many biological reactions [55]. A previous report [11] showed that synaptic plasticity requires increased intracellular calcium in the post-synaptic neuron. In some cell types, the source of calcium is influx via the NMDA receptors, and in other cell types the source of calcium is influx via the voltage-dependent calcium channels [56]. There are many calcium-binding molecules associated with synaptic plasticity, all of which bind to the calcium-calmodulin-dependent protein kinase type 2 (CaMK II) to produce LTP [57]. A previous study found that phosphorylated PKC (p-PKC) can phosphorylate GAP-43 and trigger the disaggregation of CaM from GAP-43, and the disaggregated CaM further activates CaMK II. Therefore, PKC, GAP-43, and CaM constitute a closely associated network.

A previous study [58] showed that with knock-out of the CaMK II gene, the spatial learning capacity of rats was significantly decreased, and the spatial learning capacity was damaged in CaMK II gene-mutated rats. In this study, the CaMK II levels were significantly decreased in the SCD model rats compared to normal rats, which suggests that the cognitive impairment of SCD rats is correlated with decreased levels of CaMK II. PKC activity was also decreased in SCD model rats. Therefore, we hypothesized that the decreased PKC activity causes the CaMK II levels to decrease through Ca/CaMK signal transduction, further affecting LTP. We also observed that the anti-convulsant drug LEV enhances PKC activity and CaMK II levels, which improves LTP via increasing the phosphorylation of PKC and increasing the CaMK II levels. Furthermore, the effects of LEV on PKC activity and CaMK II expression may also be closely associated with post-synaptic membrane receptors such as NMDA receptor and AMPA receptor.

Although this study obtained some interesting results, it also has a few limitations. First, we used both VPA and LEV in this study, but VPA seems to be ineffective for cognitive function improvement. In contrast to our findings, a previous study [24] reported that VPA plays an anti-epileptic role by enhancing inhibitory neurotransmitters. Further research is needed on the effects of VPA on cognitive function. Second, we did not perform dose-response curve experiments for drug dosages selection, and the optimal concentrations were consistent with the previous studies [29,30]. In future research, we plan to investigate the effects of VPA and LEV on cognitive functions. Third, this study was conducted using rats, and our results cannot be extrapolated to humans. In the future, we plan to assess the efficacy of LEV in humans. Finally, the present study did not show the direct effects of LEV on CaMK II and PKC. In the future research, we would like to investigate the effects of LEV on both CaMK II and PKC.

References:

1. Bu W, Zhao WQ, Li WL et al: Neuropeptide Y suppresses epileptiform discharges by regulating AMPA receptor GluR2 subunit in rat hippocampal neurons. *Mol Med Rep*, 2017; 16: 387–95
2. Aldenkamp AP, Beitler J, Arends J et al: Acute effects of subclinical epileptiform EEG discharges on cognitive activation. *Funct Neurol*, 2005; 20: 23–28
3. Kasteleijn-Nolst Trenite DG, Vermeiren R: The impact of subclinical epileptiform discharges on complex tasks and cognition: Relevance for aircrew and air traffic controllers. *Epilepsy Behav*, 2005; 6: 31–34
4. Nenadovic V, Stokic M, Vukovic M et al: Cognitive and electrophysiological characteristics of children with specific language impairment and subclinical epileptiform electroencephalogram. *J Clin Exp Neuropsychol*, 2014; 36: 981–91
5. Bergstrom RA, Choi JH, Manduca A et al: Automated identification of multiple seizure-related and interictal epileptiform event types in the EEG of mice. *Sci Rep*, 2013; 3: 1483
6. Garcia-Penas JJ: Interictal epileptiform discharges and cognitive impairment in children. *Rev Neurol*, 2011; 52(Suppl. 1): S43–52
7. Holmes GL, Lenck-Santini PP: Role of interictal epileptiform abnormalities in cognitive impairment. *Epilepsy Behav*, 2006; 8: 504–15
8. Lothman EW, Williamson JM: Influence of electrical stimulus parameters on afterdischarge thresholds in the rat hippocampus. *Epilepsy Res*, 1992; 13: 205–13
9. Wang Q, Wang Z, Zhu P et al: Effects of subconvulsive electrical stimulation to the hippocampus on emotionality and spatial learning and memory in rats. *Chin Med J (Engl)*, 2003; 116: 1361–65
10. Bliss TV, Gardner-Medwin AR: Long-lasting potentiation of synaptic transmission in the dentate area of the unanaesthetized rabbit following stimulation of the perforant path. *J Physiol*, 1973; 232: 357–74
11. Malenka RC, Bear MF: LTP and LTD: An embarrassment of riches. *Neuron*, 2004; 44: 5–21
12. Price R, Salavati B, Graff-Guerrero A et al: Effects of antipsychotic D2 antagonists on long-term potentiation in animals and implications for human studies. *Prog Neuropsychopharmacol Biol Psychiatry*, 2014; 54: 83–91
13. Skog MS, Nystedt J, Korhonen et al: Expression of neural cell adhesion molecule and polysialic acid in human bone marrow-derived mesenchymal stromal cells. *Stem Cell Res Ther*, 2016; 7: 113
14. Kawashima R, Ohnuma T, Shibata N et al: No genetic association between postsynaptic density-95 gene polymorphisms and schizophrenia. *Neurosci Lett*, 2006; 400: 168–71
15. Ehlis AC, Bauernschmitt K, Dresler T et al: Influence of a genetic variant of the neuronal growth associated protein Stathmin 1 on cognitive and affective control processes: An event-related potential study. *Am J Med Genet B Neuropsychiatr Genet*, 2011; 156B: 291–302
16. Zhang Z, Zhang H, Du B et al: Neonatal handling and environmental enrichment increase the expression of GAP-43 in the hippocampus and promote cognitive abilities in presatally stressed rat offspring. *Neurosci Lett*, 2012; 522: 1–5
17. Yuan Y, Sun Z, Chen Y et al: Prevention of remifentanyl induced postoperative hyperalgesia by dexmedetomidine via regulating the trafficking and function of spinal NMDA receptors as well as PKC and CaMK II level *in vivo* and *in vitro*. *PLoS One*, 2017; 12: e0171348
18. Ashpole NM, Song W, Brustovetsky T et al: Calcium/calmodulin-dependent protein kinase II (CaMK II) inhibition induces neurotoxicity via dysregulation of glutamate/calcium signaling and hyperexcitability. *J Biol Chem*, 2012; 287: 8495–506
19. Zalewska T, Domanska-Janik K: Brain ischaemia transiently activates Ca2+/calmodulin-independent protein kinase II. *Neuroreport*, 1996; 7: 637–41
20. Liu JX, Liu Y, Tang FR: Pilocarpine-induced status epilepticus alters hippocampal PKC expression in mice. *Acta Neurobiol Exp (Wars)*, 2011; 71: 220–32
21. Yabuki Y, Nakagawasai O, Moriguchi S et al: Decreased CaMK II and PKC activities in specific brain regions are associated with cognitive impairment in neonatal ventral hippocampus-lesioned rats. *Neuroscience*, 2013; 234: 103–15
22. Sadeghian H, Motiei-Langroudi R: Comparison of Levetiracetam and sodium Valproate in migraine prophylaxis: A randomized placebo-controlled study. *Ann Indian Acad Neurol*, 2015; 18 45–48
23. Sala-Padro J, Toledo M, Santamarina E et al: Levetiracetam and valproate retention rate in Juvenile myoclonic epilepsy. *Clin Neuropharmacol*, 2016; 39: 299–301
24. Geng H, Wang C: Efficacy and safety of oxcarbazepine in the treatment of children with epilepsy: A meta-analysis of randomized controlled trials. *Neuropsychiatr Dis Treat*, 2017; 13: 685–95
25. Farooq MU, Bhatt A, Majid A et al: Levetiracetam for managing neurologic and psychiatric disorders. *Am J Health Syst Pharm*, 2009; 66: 541–61
26. Mobasher MA, Sajedianfard J, Jamshidzadeh A et al: The effects of tramadol on norepinephrine and MHPG releasing in locus coeruleus in formalin test in rats: A brain stereotaxic study. *Iran J Basic Med Sci*, 2014; 17: 419–25
27. Gyengesi E, Calabrese E, Sherrier MC et al: Semi-automated 3D segmentation of major tracts in the rat brain: Comparing DTI with standard histological methods. *Brain Struct Funct*, 2014; 219: 539–50

Conclusions

Our results show that cognitive impairment occurs in the SCD rat model. The NCAM and GAP-43 levels were significantly increased and PSD-95 levels were decreased in SCD rats, and LEV treatment significantly improved these protein levels. Meanwhile, the PKC activity and CaMK II levels decreased in SCD rats, and LEV treatment significantly increased the protein levels. Therefore, we conclude that cognitive impairment in SCD model rats may be caused by decreased PKC activity, underexpression of CaMK II, and inhibition of LTP formation. LEV can improve cognitive function by activating the PKC-GAP-43-CaMK signal transduction pathway. Our results show that LEV has promise for improving cognitive function in subclinical epileptiform discharge patients.

Conflict of interest

None.

28. Racine RJ: Modification of seizure activity by electrical stimulation. II. Motor seizure. *Electroencephalogr Clin Neurophysiol*, 1972; 32: 281–94
29. van Vliet EA, Edelbroek PM, Gorter JA: Improved seizure control by alternating therapy of levetiracetam and valproate in epileptic rats. *Epilepsia*, 2010; 51: 362–70
30. Nissen-Meyer LS, Svalheim S, Tauboll E et al: Levetiracetam phenytoin, and valproate act differently on rat bone mass, structure, and metabolism. *Epilepsia*, 2007; 48: 1850–60
31. Golub MS, Germann SL, Lloyd KC: Behavioral characteristics of a nervous system-specific erbB4 knock-out mouse. *Behav Brain Res*, 2004; 153: 159–70
32. Tian Z, Ren N, Wang J et al: Ginsenoside ameliorates cognitive dysfunction in type 2 diabetic goto-kakizaki rats. *Med Sci Monit*, 2018; 23: 3922–28
33. Rozas C, Loyola S, Ugarte G et al: Acutely applied MDMA enhances long-term potentiation in rat hippocampus involving D1/D5 and 5-HT2 receptors through a polysynaptic mechanism. *Eur Neuropsychopharmacol*, 2012; 22: 584–95
34. Schulz PE, Cook EP, Johnston D: Changes in paired-pulse facilitation suggest presynaptic involvement in long-term potentiation. *J Neurosci*, 1994; 14: 5325–37
35. Lledo PM, Zhang X, Sudhof TC et al: Postsynaptic membrane fusion and long-term potentiation. *Science*, 1998; 279: 399–403
36. VanDeMark KL, Guizzetti M, Giordano G et al: The activation of M1 muscarinic receptor signaling induces neuronal differentiation in pyramidal hippocampal neurons. *J Pharmacol Exp Ther*, 2009; 329: 532–42
37. Polosa C, Teare JL, Wyszogrodski I: Slow rhythms of sympathetic discharge induced by convulsant drugs. *Can J Physiol Pharmacol*, 1972; 50: 188–94
38. Zhang L, Zhao M, Sui RB: Cerebellar fastigial nucleus electrical stimulation alleviates depressive-like behaviors in post-stroke depression rat model and potential mechanisms. *Cell Physiol Biochem*, 2017; 41: 1403–12
39. Li J, Zhou J, Wan Y et al: Association between ABO blood type and postoperative cognitive dysfunction in elderly patients undergoing unilateral total hip arthroplasty surgery in China. *Med Sci Monit*, 2017; 23: 2584–89
40. Wu P, Hong S, Zhong M et al: Effect of sodium valproate on cognitive function and hippocampus of rats after convulsive status epilepticus. *Med Sci Monit*, 2016; 22: 5197–205
41. Koo DL, Hwang KJ, Kim D et al: Effects of levetiracetam monotherapy on the cognitive function of epilepsy patients. *Eur Neurol*, 2013; 70: 88–94
42. Sanchez PE, Zhu L, Verret L et al: Levetiracetam suppresses neuronal network dysfunction and reverses synaptic and cognitive deficits in an Alzheimer's disease model. *Proc Natl Acad Sci USA*, 2012; 109: E2895–903
43. Blackwell KT, Jedrzejewska-Szmeck J: Molecular mechanisms underlying neuronal synaptic plasticity: Systems biology meets computational neuroscience in the wilds of synaptic plasticity. *Wiley Interdiscip Rev Syst Biol Med*, 2013; 5: 717–31
44. Whitlock JR, Heynen AJ, Shuler MG et al: Learning induces long-term potentiation in the hippocampus. *Science*, 2006; 313: 1093–97
45. Kolb B, Whishaw IQ: Brain plasticity and behavior. *Annu Rev Psychol*, 1998; 49: 43–64
46. Sato K, Iwai M, Nagano I et al: Temporal and spatial changes of highly polysialylated neural cell adhesion molecule immunoreactivity in amygdala kindling development. *Neurol Res*, 2003; 25: 79–82
47. Guterman A, Richter-Levin G: Neuromodulators of LTP and NCAMs in the amygdala and hippocampus in response to stress. *EXS*, 2006; 98: 137–48
48. Kleene R, Mzoughi M, Joshi G et al: NCAM-induced neurite outgrowth depends on binding of calmodulin to NCAM and on nuclear import of NCAM and fak fragments. *J Neurosci*, 2010; 30: 10784–98
49. Jia TM, Liu T, Luan B et al: [Effects of levetiracetam on the expression of NCAM and GAP-43 mRNA in the hippocampus of rats with epilepsy.] *Zhongguo Dang Dai Er Ke Za Zhi*, 2011; 13: 428–31 [in Chinese]
50. Yoshii A, Sheng MH, Constantine-Paton M: Eye opening induces a rapid dendritic localization of PSD-95 in central visual neurons. *Proc Natl Acad Sci USA*, 2003; 100: 1334–39
51. Elias GM, Elias LA, Apostolides PF et al: Differential trafficking of AMPA and NMDA receptors by SAP102 and PSD-95 underlies synapse development. *Proc Natl Acad Sci USA*, 2008; 105: 20953–58
52. Ehrlich I, Malinow R: Postsynaptic density 95 controls AMPA receptor incorporation during long-term potentiation and experience-driven synaptic plasticity. *J Neurosci*, 2004; 24: 916–27
53. Benowitz LI, Routtenberg A: GAP-43: An intrinsic determinant of neuronal development and plasticity. *Trends Neurosci*, 1997; 20: 84–91
54. Meberg PJ, Barnes CA, McNaughton BL et al: Protein kinase C and F1/GAP-43 gene expression in hippocampus inversely related to synaptic enhancement lasting 3 days. *Proc Natl Acad Sci USA*, 1993; 90: 12050–54
55. Li Q, Zhang R, Lu CL et al: [The role of subtypes of voltage-gated K⁺ channels in pulmonary vasoconstriction induced by 15-hydroeicosatetraenoic acid.] *Yao Xue Xue Bao*, 2006; 41: 412–17 [in Chinese]
56. Fino E, Paille V, Cui Y et al: Distinct coincidence detectors govern the corticostriatal spike timing-dependent plasticity. *J Physiol*, 2010; 588: 3045–62
57. Lisman J, Yasuda R, Raghavachari S: Mechanisms of CaMK II action in long-term potentiation. *Nat Rev Neurosci*, 2012; 13: 169–82
58. Battaini F, Pascale A: Protein kinase C signal transduction regulation in physiological and pathological aging. *Ann NY Acad Sci*, 2005; 1057: 177–92